PHYSICAL REVIEW A

GENERAL PHYSICS

THIRD SERIES, VOLUME 37, NUMBER 10 MAY 15, 1988

Semianalytic study of diamagnetism in a degenerate hydrogenic manifold

U. Fano and F. Robicheaux

Department of Physics and James Franck Institute, University of Chicago, Chicago, Illinois 60637

A. R. P. Rau

Department of Physics and Astronomy, Louisiana State University, Baton Rouge, Louisiana 70803

(Received 15 July 1987; revised manuscript received 17 December 1987)

The occurrence of resonant states in regions of high potential, inferred from experiments over two decades, is traced to a familiar aspect of the diagonalization of finite Hamiltonian matrices. The diagonalization generates two sets of eigenstates localized in regions of high and low potential, respectively. These sets are related by a conjugation transformation that determines the relative numbers of set elements and the scale ratio of their eigenvalue spectra. The residual eigenstates are not localized.

I. INTRODUCTION

The rapid expansion of the study of Rydberg spectra in a magnetic field stems in part from their role as prototypes for phenomena with nonseparable variables throughout chemical physics. These spectra display the transition from the spherical symmetry of an ionic field, which prevails in lower Rydberg levels, to the cylindrical symmetry imposed by a magnetic field which prevails near and beyond the ionization threshold.[1] Analogous symmetry changes accompany the evolution from the united to the separate-atom limit of a chemical bond or from a collision complex to its dissociated fragments.

Photoelectrons ejected in a magnetic field propagate mainly along **B**, with subsidiary transverse ("Landau") excitations whose spectrum has been resolved only for detachment from negative ions.[2] The Landau levels are separated by the cyclotron frequency ω_c, with orbital radii of hundreds of bohrs at fields ~ 5 T. [Stronger, astrophysical ($\sim 10^6$ T) fields confine electron motions even in ground states allowing only minor manifestations of central symmetry;[3] weaker fields, much less than 1 T, confine the symmetry evolution within an exceedingly narrow spectral range astride the ionization threshold.]

Attention has centered on prominent series of "quasi-Landau" metastable excitations whose spectral intervals evolve from the Rydberg sequence toward ω_c and whose amplitudes decay above the ionization threshold.[4] These excitations are localized astride the symmetry plane orthogonal to **B** through the ionic core. Their metastability, surprising for location on a "potential ridge" where the diamagnetic potential

$$(e^2/8mc^2)B^2r^2\sin^2\theta$$

is largest, has been attributed to an ill-defined approximate constant of the motion of a Rydberg electron in the magnetic field. Early efforts to identify its origin in the electron's dynamics near the symmetry plane have met with only limited success.[5]

The localization of quasi-Landau states has nevertheless been documented by numerical diagonalization of the relevant Hamiltonian matrix in the very large ($\gtrsim 10^3$) bases required to represent the electron over a large volume.[6] Remarkably, the localization has also emerged from calculations within modest bases consisting of a single degenerate hydrogenic manifold with a given principal quantum number n.[7] Eigenstates of diamagnetic energy thus selected by a degenerate *perturbation* treatment were shown more recently to remain approximate eigenstates of the complete Hamiltonian even for large B values, thus documenting the existence of a quasigood quantum number K.[8] The metastability represented by K breaks down eventually,[9] as anticipated by high-resolution spectroscopy very near the ionization threshold.[10] Tracing its dynamical origin constitutes the objective of the present paper. Similar goals have been pursued by previous semianalytic degenerate perturbation treatments leading only to limited results.[11]

We thus confine our scope to the matrix diagonalization of the diamagnetic energy proportional to $r^2\sin^2\theta$ within degenerate hydrogenic manifolds with given n. We shall also deal explicitly mainly with $m=0$ states, which have axial symmetry about the field **B**; their features are shared by states with $0<m\ll n$, though *not* by large-m states with $n-m\ll n$. The latter would experience a strong centrifugal field which imposes a cylindrical symmetry even for $B=0$. The transition of m/n from ~ 0 to ~ 1 will not be treated here.

As a preliminary, Fig. 1 plots eigenvalues of the diamagnetic energy matrix for different values of n. The ordinates ε_N are scaled to remove the simple n^4 dependence of $\langle r^2\rangle$ in a Coulomb potential, whereby $0\le\varepsilon_N\le\frac{5}{4}$ for all n. The abscissas N could have been similarly scaled in terms of $0<2N/n\le 1$, thus bringing all of the

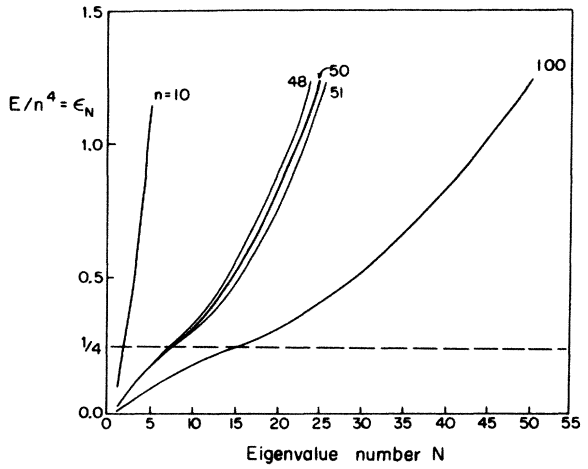

FIG. 1. Eigenvalues ε_N of the diamagnetic energy matrix (4) for $m=0$, even parity and different values of n, in dimensionless units. The index N varies in steps of unity but the eigenvalues are displayed as continuous functions. Eigenvalue curves for consecutive values of $n \gg 1$ cluster in pairs (e.g., for $n=47$ and 48, 49, and 50, etc.) (Ref. 7). Curves for each pair are not drawn separately, for clarity; they would depart from each other slightly only in the intermediate range of N.

curves into approximate coincidence. (The factor of 2 reflects the separate diagonalizations of even- and odd-l eigenstates.)

We view the eigenvalue curve for each n as consisting of *two branches* of opposite curvature, whose end points correspond to states localized astride the ridge ($\varepsilon_N \sim \frac{1}{4}$, quasi-Landau) and in the potential valley ($\varepsilon_N \sim 0$, Landau). The top branch could be brought to coincide approximately with the lower one by contracting its ordinates by a factor of 4 and its abscissas by a factor of 2. The two branches are hinged at the point of inflection [$\varepsilon_N = \frac{1}{4}$, $N = n/(2\times 3)$], where the slope $\varepsilon_N - \varepsilon_{N-1}$ is smallest, as previously known.[12] (The eigenvalues near the inflection point correspond to states which have comparable amplitudes in the valley and on the ridge.)

Our specific objective is to interpret these features analytically to $O(1/n)$; errors of this order will be corrected in accordance with a recent paper.[13] The relationship between the two branches and their eigenvectors will also be described analytically. The diagonalization process will indeed resolve into two "conjugate"—separate but mathematically similar—procedures for $\varepsilon_N \lesseqgtr \frac{1}{4}$ (Sec. III C). This similarity forces a change of perception away from considering the mechanisms underlying the formation of Landau and quasi-Landau states as independent.

The localization of eigenvectors of the diamagnetic energy will be represented by the superposition of degenerate hydrogen states $f_{nl}(r)P_{lm}(\theta)e^{im\phi}$, with given n and $m \ll n$,

$$\Psi(r,\theta) = \sum_l a_l f_{nl}(r) P_{lm}(\theta) \ . \tag{1}$$

The origin of the variable θ of the associated Legendre functions lies along **B**. Besides the value of m, the parity of l is also a constant of diagonalization. The coefficients a_l are components of each eigenvector of the matrix. Localization of quasi-Landau eigenstates astride the plane orthogonal to **B** will emerge from constructive interference of low-l components of (1) at $\theta \sim 90°$. The Landau states will be similarly localized at $\theta \sim 0°$ and 180° in terms of the *same* low-l components.

The diagonalization of the tridiagonal matrix of diamagnetic energy may be cast as a difference equation in the eigenvectors a_l.[11] This equation may be embedded in turn into standard differential equations which display qualitative features of the problem and of its solution more transparently. Section IV will describe the embedding procedure in some detail in view of its possible further applications.

The scope of this paper is confined to the treatment of a degenerate hydrogenic manifold, as noted above. Section V will, however, comment on its relevance to the realistic diamagnetism of Rydberg atoms and to broader questions of chemical physics.[14]

II. PERTURBATION MATRIX

The diamagnetic component of the magnetic energy of a Rydberg electron, quadratic in the field strength B, will be represented by $\frac{1}{2}r^2\sin^2\theta$, omitting a factor $(e^2/4mc^2)B^2$. We consider here its matrix representation in the basis of polar coordinate quantum numbers $\{n,l,m\}$, where the contributions of r^2 and $\sin^2\theta$ factor out. Analytical features of the matrix are particularly obvious in this representation. Only the submatrix diagonal in n is relevant to our degenerate perturbation treatment. The whole matrix is diagonal in m.

The nonzero matrix elements of $\sin^2\theta$ are

$$(lm \mid \sin^2\theta \mid lm) = \frac{1}{2}\left[1 + \frac{m^2 - \frac{1}{4}}{l(l+1) - \frac{3}{4}}\right] , \tag{2a}$$

$$(l-1,m \mid \sin^2\theta \mid l+1,m) = -\tfrac{1}{4}[1-(2l+1)^{-2}][1-(l+\tfrac{1}{2})^{-2}]^{-1/2} \times \left[1 - \frac{m^2}{l^2}\right]^{1/2}\left[1 - \frac{m^2}{(l+1)^2}\right]^{1/2} . \tag{2b}$$

These two expressions converge rapidly to their respective limits for $l \to n-1 \gg 1$ ($\frac{1}{2}$ and $-\frac{1}{4}$) provided $m \ll n$. A notable feature lies, for $m=0$, in the jump of (2a) from its value $\frac{2}{3}$, at $l=0$, to its next value (of equal parity) at $l=2$, namely, $\frac{10}{21} \lesssim \frac{1}{2}$; this single sharp variation of (2a) as a function of l depresses the ratio a_0/a_2 in the eigenvectors.

The corresponding nonzero matrix elements of r^2 are, in a.u.,

$$(nl \mid r^2 \mid nl) = n^4\left[1 + \frac{1}{2n^2} + \frac{3}{2}\left[1 - \frac{l(l+1)}{n^2}\right]\right] , \tag{3a}$$

$$(n,l-1 \mid r^2 \mid n,l+1) = n^4\frac{5}{2}\left[1 - \frac{l^2}{n^2}\right]^{1/2}\left[1 - \frac{(l+1)^2}{n^2}\right]^{1/2} . \tag{3b}$$

The expressions in large square brackets are cast so as to stress the evolution from their value at $l=0$ to the limit $l \to n-1 \gg 1$. In this limit the bracketed term of (3a) approaches unity while (3b) vanishes. In the opposite limit, $l=0$, and for $n \gg 1$, both expressions (3) reduce to $n^4 5/2$. Note that the difference n^2-l^2 in (3) represents the squared magnitude of the Lenz vector. The similarity in form of the radial matrix elements in (3) to the angular ones in (2) stems from the O(2,1) symmetry of hydrogenic radial functions.[15] The algebraic structure of O(2,1) closely parallels that of the O(3) for angular momentum.

Multiplication of (2) and (3) yields only two nonzero matrix elements, functions of l which depend on parameters n and m,

$$V_l=(nlm \mid \tfrac{1}{2}r^2\sin^2\theta/n^4 \mid nlm)=\frac{1}{4}\left[1+\frac{1}{2n^2}+\frac{3}{2}\left[1-\frac{l(l+1)}{n^2}\right]\right]\left[1+\frac{m^2-\frac{1}{4}}{l(l+1)-\frac{3}{4}}\right], \quad |m| \le l < n \tag{4a}$$

$$\begin{aligned} W_l&=(n,l-1,m \mid \tfrac{1}{2}r^2\sin^2\theta/n^4 \mid n,l+1,m) \\ &=-\frac{5}{16}\left[1-\frac{l^2}{n^2}\right]^{1/2}\left[1-\frac{(l+1)^2}{n^2}\right]^{1/2}[1-(2l+1)^{-2}][1-(l+\tfrac{1}{2})^{-2}]^{-1/2}\left[1-\frac{m^2}{l^2}\right]^{1/2} \\ &\quad\times\left[1-\frac{m^2}{(l+1)^2}\right]^{1/2}, \quad |m|<l<n\ . \end{aligned} \tag{4b}$$

The limiting value of V_l at $l=n-1, \frac{1}{4}$, coincides with the ordinate of the inflection point in Fig. 1. The limiting values of both V_l and W_{l+1} for $l \neq 0$ but $l \ll n$, namely, $\frac{5}{8}$ and $-\frac{5}{16}$, will determine other features of Fig. 1.

In order to emphasize the major analytic elements of Eqs. (4), we separate their dominant terms from corrections that vanish for large l and n, to be taken into account in numerical applications, by writing

$$V_l \simeq \frac{1}{4}\left\{1+\frac{3}{2}\left[1-\left[\frac{l+\frac{1}{2}}{n}\right]^2\right]\right\}+O\left[\frac{1}{n^2}\right] +O((2l+1)^{-2})\ , \tag{4a'}$$

$$W_l \simeq \frac{5}{16}\left[1-\left[\frac{l+\frac{1}{2}}{n}\right]^2\right]+O\left[\frac{1}{n^2}\right] +O((2l+3)^{-2})\ . \tag{4b'}$$

These approximate forms are very accurate, except for small l. However, V_0 will only enter into a boundary condition where it can be handled explicitly, while V_2 and V_4 are too large by only $\sim 4\%$ and 1%, respectively.

The dependence of (4) on l through quadratic terms reflects, of course, the quadratic dependence of the magnetic energy on r and on θ. Different dependence of the energy matrix on quantum numbers should, of course, be expected in different problems but the occurrence of *low powers* of quantum numbers is probably widespread. Another illustration is provided by the more familiar linear Stark effect in a degenerate n manifold which we consider in Appendix A. Note that the perturbation generates a correlation of the radial and angular variables (r,θ). This correlation expresses itself through the coefficients a_l of (1), that is, through the probability amplitudes of alternative *partitions*

$$n=n_r+l+1 \tag{5}$$

of the total quantum number n into the radial and orbital quantum numbers that correspond to r and θ, respectively.[16]

III. DIAGONALIZATION PROCESS

The eigenvalues ε_N and the eigenvectors $a_l^{(N)}$ of the matrix (4) are determined by the linear-algebraic system

$$W_{l-1}a_{l-2}+V_l a_l+W_{l+1}a_{l+2}=\varepsilon a_l\ , \tag{6}$$

which amounts to a three-term recursion formula. Separate sets of solutions of (6) occur, with alternative parities of l, because (6) interconnects only components of the eigenvectors $\{a_l\}$ with l values of equal parity. The coefficients of (6) suffice to determine the spread of eigenvalues ε_N in Fig. 1, through the equation[17]

$$\sum_N \varepsilon_N^2-\left[\sum_N \varepsilon_N\right]^2=\sum_l{}'(V_l^2+2W_{l+1}^2)-\left[\sum_l{}' V_l\right]^2\ . \tag{7}$$

The prime indicates summation over l values of the same parity.

The finite range of l values, indicated in (4b), causes the two relations (6) with lowest and highest values of l to consist of only two nonzero terms, namely,

$$(V_{|m|}-\varepsilon)a_{|m|}+W_{|m|+1}a_{|m|+2}=0\ , \tag{8a}$$

$$W_{n-2}a_{n-3}+(V_{n-1}-\varepsilon)a_{n-1}=0\ . \tag{8b}$$

[All indices of (8a) may be raised by unity and/or those of (8b) reduced by unity, depending on the parity of $l-m$ and of $n-l$, respectively.] Equations (8) set the ratios of the first two and of the last two elements of the recursion (6), respectively. The three-term recursion (6) then determines the ratios of the successive elements a_l to the first and last elements of their sequence. Compatibility of these separate sets of ratios would finally select the eigenvalues ε_N in a numerical solution.

To obtain a semianalytic solution of (6) we shall instead recast (6) as a difference equation analogous to the one-dimensional wave equation $d^2y/dx^2+k^2(x)y(x)=0$, a

procedure utilized previously in Ref. 11(c). The analog of $k^2(x)$ will illustrate the features of Fig. 1 and of the corresponding a_l.

A. Difference equation

We define the second difference of the eigenvector components a_l as

$$\delta^{(2)}a_l=(a_{l+2}-2a_l+a_{l-2})/4 , \tag{9}$$

where the coefficient $\frac{1}{4}$ stems from l varying in steps of 2. The terms of (6) with W coefficients are thus expressed in terms of $\delta^{(2)}a$ as

$$\begin{aligned} W_{l-1}a_{l-2}+W_{l+1}a_{l+2}=&\tfrac{1}{2}(W_{l-1}+W_{l+1})(4\delta^{(2)}a_l+2a_l) \\ &+\tfrac{1}{2}(W_{l+1}-W_{l-1}) \\ &\times(a_{l+2}-a_{l-2}) . \end{aligned} \tag{10}$$

Casting (6) in the form $d^2y/dx^2+k^2(x)y(x)=0$ requires us to eliminate the first difference term in (10). This is accomplished by splitting a suitable factor out of a_l (following, e.g., a procedure of Ref. 13),

$$a_l=c_l A_l , \tag{11}$$

and setting

$$W_{l-1}c_{l-2}=W_{l+1}c_{l+2} , \tag{12}$$

whence follows the recursion formula

$$c_{l+4t}/c_l=\prod_{s=0}^{t-1}(W_{l+1+4s}/W_{l+3+4s}) . \tag{13}$$

Initial values of (c_0,c_2), or of (c_1,c_3), can be set to unity.

Equation (6) now takes the equivalent form

$$W_{l-1}c_{l-2}(4\delta^{(2)}A_l+2A_l)+V_l c_l A_l=\varepsilon c_l A_l , \tag{14}$$

$$\delta^{(2)}A_l+K^2(l)A_l=0 , \tag{15}$$

with

$$K^2(l)=\frac{\varepsilon-[V_l+(2W_{l-1}c_{l-2}/c_l)]}{-4W_{l-1}c_{l-2}/c_l} . \tag{16}$$

The ratios c_l/c_{l-2} in (16) calculated from (13) depart significantly from unity only for $l\sim n$ as shown in Fig. 2. A positive sign of $K^2(l)$ implies, of course, an oscillatory dependence of A_l on l, a negative sign implies an exponential dependence. Construction of an eigenvector of (15) requires at least one of the coefficients of $K^2(l)$ to be positive. Using (4a') and (4b') to $O(1/n)$, we reduce (16) to the more transparent form

$$\begin{aligned} K^2(l)=&\frac{4}{5}\frac{\varepsilon-(l^2/4n^2)}{1-(l^2/n^2)}\frac{c_l}{c_{l-2}}-\frac{1}{2}\left[\frac{c_l}{c_{l-2}}-1\right] \\ &+O((2l+1)^{-2})+O(1/n) , \end{aligned} \tag{17}$$

which forms the basis for further discussion.

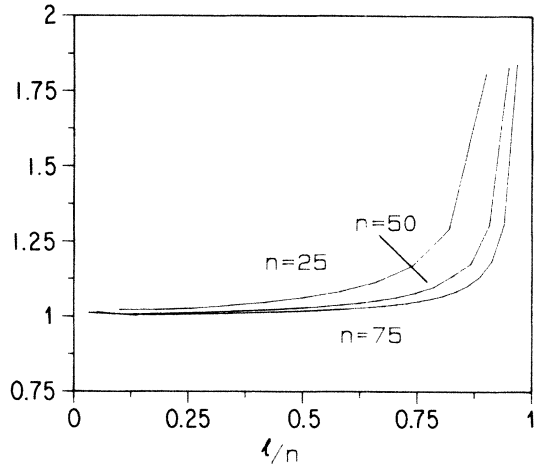

FIG. 2. Ratios c_l/c_{l-2}, Eqs. (12) and (13).

B. Lower-energy spectrum

The first and main term of the squared wave number (17) may be interpreted as

$$K^2(l)=2m^*(l)[\varepsilon-\mathcal{V}(l)]+O((2l+1)^{-2})+O(1/n) , \tag{18}$$

the product of an effective kinetic energy $\varepsilon-\mathcal{V}(l)$ and of twice an effective mass $m^*(l)$. The effective potential is defined as

$$\begin{aligned} \mathcal{V}(l)=&V_l+W_{l-1}+W_{l+1} \\ =&(l+\tfrac{1}{2})^2/4n^2+O((2l+1)^{-2})+O(1/n^2) , \end{aligned} \tag{19}$$

and the effective mass as

$$m^*(l)=\frac{1}{-4(W_{l-1}+W_{l+1})}\frac{c_l}{c_{l-2}} . \tag{20}$$

The energy eigenvalue ε in (18) must be positive so that $K^2(l)$ will not be negative throughout. The potential $\mathcal{V}(l)$ confines the eigenvector within an oscillator-type well with exponential decay for $l^2>4\varepsilon n^2$. The effective mass $m^*(l)$ diverges at $l\sim n$ thus accelerating the exponential decay for $\varepsilon<\frac{1}{4}$. The same divergence presents a major problem for $\varepsilon>\frac{1}{4}$ which we will address in Sec. III C.

The lowest-energy states have wave functions concentrated in the region of lowest diamagnetic potential, that is, along the z axis, $\theta=0°$ or 180°. Extreme concentration, represented by a superposition of two δ functions $\delta(1\pm\cos\theta)$, would cause the coefficients a_l of the wave function (1), $\Psi(r,\theta)$, to be proportional to $[(2l+1)/n]^{1/2}$ for $l-m$ even, 0 otherwise. The concentration does not actually reach such an extreme but spreads around $\theta=0°$ or 180° in the form of a Gaussian in θ. This translates, through a Fourier transform, into a Gaussian function of l, namely,

$$a_l=(\tfrac{4}{5})^{1/4}[(2l+1)/n]^{1/2}\exp[-l(l+1)/2\sqrt{5}n] . \tag{21}$$

Note that the effective range of l is proportional to $\sqrt{n}$, as in random walk problems.

On the basis of (17) the lowest few eigenvalues are represented by

$$\varepsilon_N=\frac{\sqrt{5}}{2n}(N+\tfrac{1}{2}) , \tag{22}$$

with spacings

$$\varepsilon_{N+2}-\varepsilon_N=\sqrt{5}/n . \tag{22'}$$

The corresponding eigenvectors are in essence Hermite-type functions. This approach is valid as long as $m^*(l)$ can be replaced by $m^*(0)$. The actual increase in $m^*(l)$ increases the magnitude of $K^2(l)$ thus decreasing the spacings of successive eigenvalues in accordance with Fig. 1. Further analysis of this behavior is deferred to Sec. IV, where it will be conducted by embedding the difference equation into a differential problem.

A single further application will be carried out here to estimate the number $N_{\max}$ of eigenvalues of (15) within our immediate scope, that is, with $\varepsilon_N \le \frac{1}{4}$. This is done by evaluating the "phase sum" $\sum_l K(l)$ at $\varepsilon=\frac{1}{4}$ and setting it equal to $N_{\max}\pi$. We disregard, however, the terms of lower order as well as the ratio c_l/c_{l-2}, at least initially. In accordance with the definition (9), the "phase sum" extends over all values of l and yields

$$\sum_l K(l)\,|_{\varepsilon=1/4}=n/\sqrt{5}=N_{\max}\pi . \tag{23}$$

The result,

$$N_{\max}=0.285n/2 , \tag{24}$$

will turn out low by 15%,[18] which would be compensated, at least in part, by including in $K(l)$ the contribution of $(c_l/c_{l-2})^{1/2}>1$.

C. Upper energy spectrum: Conjugation

The first term of (17), which is large and negative for $\varepsilon<\frac{1}{4}$ and $l\sim n$, becomes large and positive for $\varepsilon>\frac{1}{4}$ and $l\sim n$. The implications of such large values of $K^2(l)$ for the eigenvectors A_l are not readily assessed by inspection of (15). This equation must then be recast once again into a more transparent form by an orthogonal transformation, which leaves its spectrum invariant.

An appropriate transformation consists simply of sign reversal of alternate elements of the sets $\{a_l\}$ and $\{A_l\}$, represented by the substitutions

$$a_l=(-1)^{[l/2]}b_l, \quad A_l=(-1)^{[l/2]}B_l , \tag{25}$$

where $[l/2]$ equals $l/2$ when l is even and $(l-1)/2$ when it is odd. The transformation (25) is analogous to those that interchange electron eigenstates near the top of a band with those near its bottom, or interchange occupied and vacant states in a partially filled atomic subshell.[19] This transformation will be seen to interchange the sets of solutions of (15) with $\varepsilon<\frac{1}{4}$ and with $\varepsilon>\frac{1}{4}$. It will also be seen to interchange some of the major characteristics of the two subsets and will be referred to as a conjugation. It will not, however, conserve the number of eigenvalues nor their range of values. Note that the point $\varepsilon=\frac{1}{4}$ acts as a "separatrix" between the conjugate subsets of eigenstates; it corresponds to $\Lambda=0$, where $\Lambda=4\mathbf{A}^2-5A_z^2$ in terms of the Lenz vector $\mathbf{A}$, is a parameter introduced in earlier semianalytic treatments.[11(a)]

The transformation (25) applies on both sides of the matrix operator in (4) and (6), thus *reversing* the sign of each of its *off-diagonal* elements $W_{l\pm1}$ while leaving the *diagonal* V_l *unchanged.* [Note, incidentally, that the sign reversal of the W affects neither of the spectral parameters (7), as expected.] The linear Stark effect considered in the Appendix, where the diagonal V_l vanish identically, affords an example where the transformation analogous to (25), together with $\varepsilon\to-\varepsilon$, leaves (6) unchanged; pairs of eigenvalues $\pm\varepsilon$ differ only in having an alternation in sign of the l components in their eigenvectors.

To discuss the effect of this transformation, we extend the definition of $K^2(l)$ in (16) to read

$$K_{\pm}^2(l)=\frac{\varepsilon-[V_l\pm(2W_{l-1}c_{l-2}/c_l)]}{\mp4W_{l-1}(c_{l-2}/c_l)} , \tag{26}$$

with the understanding that the upper sign applies to the states with $\varepsilon<\frac{1}{4}$ and the lower sign applies to those with $\varepsilon>\frac{1}{4}$. The analog of (17) is

$$K_-^2(l)=\frac{4}{5}\frac{\frac{5}{4}-\varepsilon-(l^2/n^2)}{1-(l^2/n^2)}\frac{c_l}{c_{l-2}}-\frac{1}{2}\left[\frac{c_l}{c_{l-2}}-1\right]+O((2l+1)^{-2})+O\left[\frac{1}{n}\right] . \tag{27}$$

This expression may be interpreted in analogy to Sec. III B by extending Eqs. (19) and (20) to

$$\mathcal{V}_{\pm}(l)=V_l\pm W_{l-1}\pm W_{l+1} , \tag{28}$$

$$m_{\pm}^*(l)=\frac{1}{\mp(W_{l-1}+W_{l+1})}\left[\frac{c_l}{c_{l-2}}\right] , \tag{29}$$

whereby

$$\mathcal{V}_-(l)=\tfrac{5}{4}-\left[l+\frac{1}{2}\right]^2/n^2+O((2l+1)^{-2})+O\left[\frac{1}{n^2}\right] , \tag{30}$$

which corresponds to an inverted oscillator.

The energy eigenvalue ε in (27) must be less than $\frac{5}{4}$ so that $K_-^2(l)$ will not be negative throughout. Also ε cannot be less than $\frac{1}{4}$ since $K_-^2(n)$ would become large and positive. The allowed range of ε is thus four times larger than in Sec. III B, as expected from Fig. 1. The same factor of 4 represents the ratio of the coefficients in the numerators of (18) and (27) and thus determines the ratio of the ranges of $\mathcal{V}_-$ and $\mathcal{V}_+$ in Fig. 3.

The solutions of Eq. (15) with K_-^2 given by (27) is thus represented by Hermite-type functions analogous to the solutions for K_+^2 except for a factor of 2 in the scale of their effective frequencies. Indeed, the *slopes* of the plots of ε_N in Fig. 1 are twice as large at $\varepsilon_N\sim\frac{5}{4}$ than at $\varepsilon_N\sim0$. The *number* of eigenvalues in the range $\frac{1}{4}<\varepsilon<\frac{5}{4}$ is also boosted by a factor of 2 since the $N_{\max}$ evaluated by (24) is proportional to $[K_-(l)]_{\varepsilon=1/4}$ rather than to its square. Combining the numbers of eigenvalues thus estimated by

(24) for $\varepsilon < \frac{1}{4}$ with the twice-larger corresponding number estimated here for $\varepsilon > \frac{1}{4}$, we obtain the total of 0.85 $(n/2)$, 15% short of the value $N/2$ which corresponds to the size of the matrix.[18] The conjugation transformation (25) has thus separated the solution of (6) into two equivalent problems with eigenvalues $\varepsilon \lessgtr \frac{1}{4} = \lim_{l\to n} V_l$, respectively.

We discuss next the striking correspondence of the angular distributions represented by the eigenfunctions (1) for the lower and upper ranges of eigenvalues, specifically for the strongly localized states of each group with the lowest or highest eigenvalues. The eigenvector components $\{A_l\}$ and $\{B_l\}$ of these states decrease exponentially with increasing l for $l > l_0 = O(\sqrt{n})$. The spherical harmonics $P_{lm}(\theta)$, with $l < l_0$, have positive values over a range $0 < \theta \leq 1/(l - |m|)$ and thus contribute *additively* to

$$\Psi = \sum_l a_l f_{nl}(r) P_l(\cos\theta)$$

throughout this range insofar as the eigencomponents

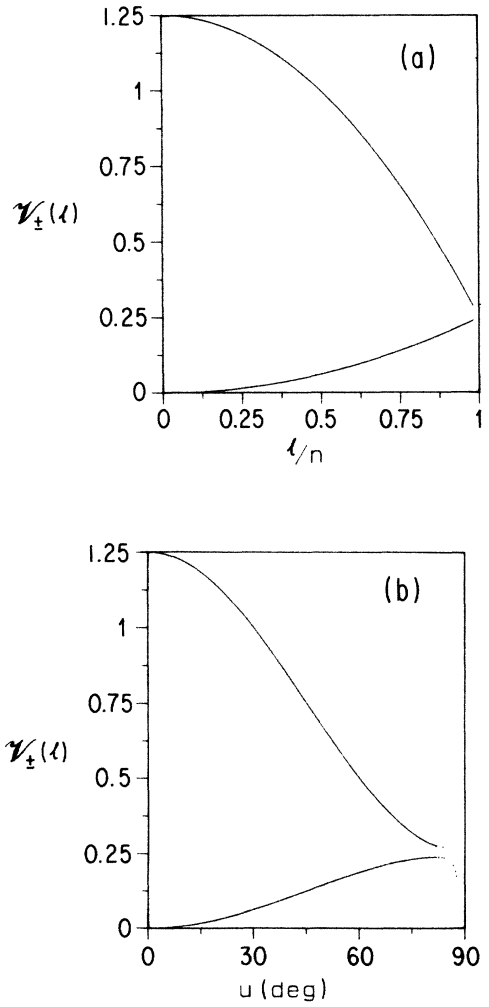

FIG. 3. Effective potentials $\mathcal{V}_l$, defined in text. (a) From Eqs. (21a) and (21b). (b) From differential Eq. (33) divided by $4n^2/5$; dotted portion of curves extends beyond the range of $l \leq n-1$.

$a_l = c_l A_l$ remain positive, as they do for the lowest-energy eigenstate. The highest-energy eigenstate is instead represented by

$$\Psi(r,\theta) = \sum_l a_l f_{nl}(r) P_{lm}(\theta)$$
$$= \sum_l c_l B_l f_{nl}(r)(-1)^{[l/2]} P_{lm}(\theta) \,. \tag{31}$$

The functions $(-1)^{[l/2]}P_{lm}(\theta)$ *alternate* in sign at $\theta \sim 0°$ according to the parity of $[l/2]$ generating a destructive interference. On the other hand, they have *equal sign* at and near $\theta = 90°$, thus contributing *additively in this range.* The conjugation transformation (25) is thus seen to *shift the localization* of $\Psi(r,\theta)$ from the proximity of $\theta \sim 0°$ to that of $\theta \sim 90°$.

Indeed, paralleling the earlier discussion leading to (21) for the low eigenvalues, the high eigenvalues reach high energy by being concentrated in directions orthogonal to the magnetic field, where the diamagnetic potential is a maximum. Extreme concentration into this direction, now represented by $\delta(\cos\theta)$, would give in (1), $a_l = [(2l+1)/n]^{1/2} P_l(0)$. Once again, however, the concentration has a spread in θ around $\theta = 90°$ and is correspondingly reflected in a Gaussian dependence on l/n

$$b_l = (2\pi/\sqrt{5}n)^{1/4}(-1)^{[l/2]} P_l(0)(2l+1)^{1/2}$$
$$\times \exp[-l(l+1)/\sqrt{5}n] \,. \tag{32}$$

Figure 4 shows that the above expression gives a good description of the eigenvectors obtained by numerical diagonalization. Note that the exponent of (32) differs by a

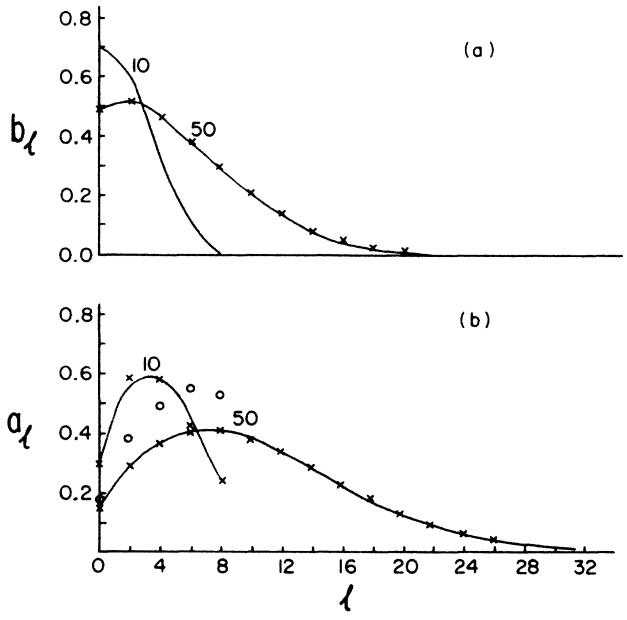

FIG. 4. Eigenvectors of the matrix (4), with $n = 10$ and 50, $m = 0$, and even parity l. (a) $b_l^{[n/2]}$; (b) $a_l^{(0)}$; ——, numerical solution of Eq. (6); ×, Eqs. (21) and (32) for $n = 10$, which approximate the results of Sec. IV closely; ○, Refs. 11(d) and 11(e).

factor of 2 from its value for the lowest eigenvectors. This difference reflects the scaling ratio of lowest and highest eigenvectors that was discussed earlier. The result in (32) means that Ψ in (31) has a Gaussian distribution around $\theta=90°$ with a width proportional to $n^{-1/2}$. The rapid exponential falloff in the contribution of high-l values ($l>l_0\propto n^{1/2}$) to the lowest and highest eigenvalues expresses, therefore, the tight concentration of $\Psi(r,\theta)$ in directions parallel and transverse to the field.

Finally, the connection of the conjugation operator (25) in our problem to the interchange of longitudinal and transverse excitations with respect to the magnetic field is clearly related to the structure of the diamagnetic potential, specifically to its $\sin^2\theta$ dependence. The transformation $\theta\rightarrow 90°-\theta$ takes $\sin^2\theta\rightarrow\cos^2\theta=1-\sin^2\theta$. The off-diagonal W_l acquire, therefore, a change in sign. For the diagonal V_l, as observed after (2a), the angular matrix element is $\simeq\frac{1}{2}$ for all l except for $l=0$. That is, $\sin^2\theta$ and $\cos^2\theta$ both contribute the same value, namely $\frac{1}{2}$, and V_l remains unchanged.

IV. EMBEDDING IN DIFFERENTIAL EQUATIONS

The basic diagonalization equations (6) and (15) approach integral and differential equations, respectively, in the limit of large n, where l/n or $n_r/n=1-(l+1)/n$ may be treated as continuous variables. This opportunity proves helpful since many equations of mathematical physics have familiar analytic solutions which display the influence of characteristic features of their coefficients, such as the simple dependence of (18) on l^2/n^2. Exploitation of this opportunity is made increasingly attractive by the recent realization that moderate nonsingular departures of equation coefficients from a standard form can be taken into account by numerical adjustment of a coordinate.[13]

In converting a difference to a differential equation, the error in the eigenvalues due to the *conversion* is of the order $(N_i/n)^2$, where N_i is the number of nodes of the eigenvector i,[18] which agrees with the level of approximation of (4a′) and (4b′) and accounts for the 15% error noted in Sec. III C. Indeed, the conjugation transformation of Sec. III C is vital to the accuracy of the higher eigenvalues by limiting the range of N_i.

For the sake of flexibility we map our discrete variable l (or n_r) on a continuous u by an initially unspecified functional relationship $l(u)$. Dealing with an eigenvalue problem requires the mapping of eigenvector components a_l on a continuous variable $a(u)$ to preserve normalization. We thus set

$$\sum_l a_l^2=\int_{u_0}^{u_1} du\, a^2(u)\ , \tag{33}$$

which implies

$$a_{l(u)}=(dl/du)^{-1/2}a(u)\ . \tag{34}$$

The difference operator $\delta^{(2)}$ is converted to a differential operator by standard methods,

$$\begin{aligned}\delta^{(2)}a&=\left[\frac{dl}{du}\right]^{-1}\frac{d}{du}\left[\frac{dl}{du}\right]^{-1}\frac{d}{du}\left[\frac{dl}{du}\right]^{-1/2}a(u)\\&=\left[\frac{dl}{du}\right]^{-5/2}\left\{a''(u)-2\frac{l''}{l'}a'(u)\right.\\&\quad\left.+\left[\frac{5}{4}\left[\frac{l''}{l'}\right]^2-\frac{1}{2}\frac{l'''}{l'}\right]a(u)\right\}\ .\end{aligned} \tag{35}$$

The remaining terms of the differential equation are adapted from (10) rather than (14) because the renormalization (11) is not convenient in the present context. On the other hand, the conjugation operator is essential and one shall obtain conjugate pairs of differential equations for the functions $a(u)$ and $b(u)$. The approximate matrix elements (4a′) and (4b′) suggest two forms of $l(u)$, namely, $l(u)=nu-\frac{1}{2}$ and $l(u)=n\sin u-\frac{1}{2}$.

The linear form simplifies (35) since all but the first derivatives of $l(u)$ vanish. The resulting equation contains a first derivative and has the form 21.6.2 of Ref. 20 for the angular prolate spheroidal function. However, the boundary conditions at $u=0$ for $a(u)$ and $b(u)$ are not the same as for the ordinary spheroidal functions, thus causing $a(u)$ and $b(u)$ and their eigenvalues to depart from the standard form (Eq. 21.7.5 of Ref. 20). Accordingly, we do not pursue this approach except for a limited application which is insensitive to boundary conditions.

The application concerns the difference of successive eigenvalues $\Delta\varepsilon_N$ for eigenfunctions with many nodes, specifically for $\varepsilon_N\sim\frac{1}{4}$. The eigenvalue λ_N in 21.6.2 of Ref. 20 is related to ε_N by $\varepsilon_N=5\lambda_N/4n^2$. The approximate formula for $\Delta\lambda_N$, $N=n/6$ gives $\Delta\varepsilon_{n/6}=0.85\sqrt{5}/2n$, which is approximately $\frac{1}{2}\Delta\varepsilon_0$ and $\frac{1}{4}\Delta\varepsilon_{n/2}$, in accordance with Fig. 1, a feature not previously identified.

The construction of the differential equation for $l(u)=n\sin u-\frac{1}{2}$ is more complicated than for the linear form but generates no first derivative term whereby the differential equation has the same structure as (15), namely,

$$a''(u)+\frac{4n^2}{5}\left[\varepsilon-\tfrac{1}{4}\sin^2u+\frac{5}{16n^2}\frac{1}{\cos^2u}\right]a(u)=0\ , \tag{36a}$$

$$b''(u)+\frac{4n^2}{5}\left[\tfrac{5}{4}-\varepsilon-\sin^2u+\frac{5}{16n^2}\frac{1}{\cos^2u}\right]b(u)=0\ , \tag{36b}$$

still to $O(1/n^2)+O((2l+1)^{-2})$ as in Sec. III. Note the following aspects of these equations.

(a) The coefficient $\frac{4}{5}$ and the main terms in the brackets coincide with the numerator of $K_{\pm}^2(l)$ in (26).

(b) The denominator $[1-(l^2/n^2)]$ of (26), representing the divergence of m^*, has been absorbed into the differential elements, a step which has also eliminated the first derivative term. The replacement of the range of l, $0\le l<n$, by that of $\sin u$ has also introduced the factor n^2

in front of the brackets.

(c) The replacement of l/n by $\sin u$ rounds off the potential in Fig. 3(b) as u approaches 90°. It also introduces the singularity $1/\cos^2 u$ which, however, only contributes to $O(1/n)$ and need not be considered explicitly here.[21]

(d) Equations (36) are periodic in u and depart from the Mathieu equation (20.1.1 of Ref. 20) only through the occurrence of the "centrifugal" term $1/\cos^2 u$.

Inspection of Eqs. (36) bears out the approximate results obtained in Sec. III. More detailed, quantitative results could be derived from information available on the Mathieu functions. However, this information is not as extensive as it is for other functions of mathematical physics. Therefore we proceed by the method of Ref. 13 fitting the solutions of (36) to parabolic cylinder functions (Ref. 20, Chap. 19) which include oscillator eigenfunctions as special cases. We restrict this calculation to the quantum number $m=0$.

According to Ref. 13, we set

$$a(u)=\left[\frac{dx(u)}{du}\right]^{-1/2}[C^e A^e(\alpha;x(u))+C^o A^o(\alpha;x(u))]\ , \tag{37}$$

where $A^{e,o}$ are the even and odd solutions of

$$\frac{d^2A}{dx^2}+[\alpha-(x^2/4)]A=0\ , \tag{38}$$

and the constant α is still to be fixed. Upon substituting (37) into (36), and using (38) to eliminate d^2A/dx^2, we find $x(u)$ to be defined by the integral equation

$$\int_0^x[\alpha-(x'^2/4)]^{1/2}dx'=\int_0^u k(u')du' \tag{39}$$

to order $(x''/x')^2$, where $k(u)$ is the effective wave number of (36) complemented by terms $O((2l+1)^{-1})$ neglected in (36). We note that taking into account the small, cumbersome corrections to (39) would be fruitless since (35) is itself an approximation. Equation (39) yields, when the integration limits x and u coincide with the zeros of the respective integrands, namely 0 and u_T,

$$\alpha=(2/\pi)\int_0^{u_T}k(u')du'\ . \tag{40}$$

Equations (36) and (40) establish a relationship between the eigenvalue ε and the parameter α which holds regardless of boundary conditions, namely,

$$\varepsilon=\frac{\sqrt{5}}{2n}\alpha-\left[\frac{25}{32n^2}\left[\frac{1}{n}+\frac{2\alpha}{\sqrt{5}}\right]^2+\frac{5}{4n^2}\right]-\frac{1}{n}\left[\frac{5-\sqrt{5}}{6}-\frac{\sqrt{5}}{2n}\alpha\right]+O\left[\frac{1}{n^3}\right]\ , \tag{41a}$$

for $\varepsilon<1/4$, and

$$\varepsilon=\frac{5}{4}-\frac{\sqrt{5}}{n}\alpha+\left[\frac{25}{32n^2}\left[\frac{1}{2n}+\frac{2\alpha}{\sqrt{5}}\right]^2+\frac{5}{4n^2}\right]+\frac{1}{n}\left[\frac{5}{4}-\frac{\sqrt{5}}{n}\alpha-\frac{5+\sqrt{5}}{6}\right]+O\left[\frac{1}{n^3}\right]\ , \tag{41b}$$

for $\varepsilon>\frac{1}{4}$. The term before the square brackets in (41) results from the approximation $\sin^2 u=u^2$, the terms in square brackets from the nonparabolic terms in (36). The last significant term represents a fit to the numerical contribution to $k(u)$ of $O((2l+1)^{-2})$.

A second relation between ε and α is established by the boundary conditions (8). The specific condition (8b), at $u=90°$, has little effect except in the vicinity of $\varepsilon=\frac{1}{4}$, where the eigenfunction penetrates substantially into the region of imaginary wave number near $u=90°$. In the use of (40) we have assumed a negligible value of the eigenfunction at $u=90°$ by using parabolic cylinder functions of Whittaker type (Ref. 20, Eqs. 19.3). According to equation 19.3 of Ref. 20, this condition restricts the coefficients of (37) by

$$\frac{C^o}{C^e}=\sqrt{2}\frac{\Gamma(\frac{3}{4}+(\alpha/2))}{\Gamma(\frac{1}{4}+(\alpha/2))}\tan\left[\alpha\frac{\pi}{2}-\frac{\pi}{4}\right]\cong\alpha^{1/2}\left[1+\frac{1}{16\alpha^2}\right]\tan\left[\alpha\frac{\pi}{2}-\frac{\pi}{4}\right]\ . \tag{42}$$

The remaining boundary condition (8a) at $u=0$ will provide a second condition on C^o/C^e, thus relating α directly to the eigenvalue ε.

The boundary condition at $u=0$ is handled by rewriting (8a) in terms of the eigenfunctions $a(u)$ and $b(u)$,

$$\left[\left[\frac{dl}{du}\right]^{-1/2}a(u)\right]_{u(2)}\Big/\left[\left[\frac{dl}{du}\right]^{-1/2}a(u)\right]_{u(0)}=1+(\varepsilon-W_1-V_0)/W_1\ , \tag{43a}$$

$$\left[\left[\frac{dl}{du}\right]^{-1/2}b(u)\right]_{u(2)}\Big/\left[\left[\frac{dl}{du}\right]^{-1/2}b(u)\right]_{u(0)}=1+(V_0-W_1-\varepsilon)/W_1\ . \tag{43b}$$

Substituting (37) and its analog for $b(u)$ into these equations and using (36), (37), (38), and the definition of parabolic cylinder functions (Ref. 20, Eqs. (19.2), we find

$$\frac{C^o}{C^e}=\left[\frac{5\alpha}{\varepsilon}\right]^{1/2}\gamma^+/(4-\gamma^+) \tag{44a}$$

for $\varepsilon<\frac{1}{4}$, and

$$\frac{C^o}{C^e}=\left[\frac{5\alpha}{\frac{5}{4}-\varepsilon}\right]^{1/2}\gamma^-/(4-\gamma^-) \tag{44b}$$

for $\varepsilon>\frac{1}{4}$, where

$$\gamma^{\pm}=\pm\frac{6}{\sqrt{5}}\left[\frac{5\mp\sqrt{5}}{6}-\varepsilon\right]\ .$$

The eigenvalues in Table I were found using (41), (42), and (44) with a hand-held calculator. Also shown are the eigenvalues found by numerical diagonalization of (6) and values of the parameter α.

TABLE I. Comparison of eigenvalues from Eqs. (41) and (6) for $n=49$.

ε		α^{a}
Eq. (41)	Eq. (6)	Eq. (40)
0.0221	0.0226	1.396
0.0641	0.0657	3.305
0.1045	0.1061	5.224
0.1430	0.1436	7.144
0.1790	0.1780	9.068
0.214	0.209	10.99
0.65	0.69	14.08
0.73	0.75	12.09
0.81	0.82	10.11
0.890	0.896	8.133
0.974	0.973	6.169
1.055	1.054	4.219
1.144	1.139	2.325
1.223	1.228	0.621

[a]These values may be compared to oscillator eigenvalues for odd parity states ($\frac{3}{2}, \frac{7}{2}, \ldots$) for $\varepsilon < \frac{1}{4}$ and for even parity ($\frac{1}{2}, \frac{5}{2}, \ldots$) for $\varepsilon > \frac{1}{4}$.

The eigenvectors constructed from (37) and (39) are shown in Fig. 4, along with those from the exact numerical diagonalization, for the lowest and highest eigenvalues, in which cases they fit closely the analytical expression (21) and (32). Earlier studies had not fully appreciated the crucial implication of (21) and (32) that only a limited range of values ($l \lesssim n^{1/2}$) contributes to the eigenvectors near either limit, $\varepsilon=0$ and $\varepsilon \sim \frac{1}{4}$. Analytical expressions proposed in Refs. 11(d) and 11(e) and based on studies of diamagnetism through O_4 symmetry do not describe the eigenvectors well. Figure 4 compares the coefficients given by Refs. 11(d) and 11(e) for the lowest eigenvector with our (21) and with the results of numerical diagonalization. Corresponding results for the lowest eigenvalue are 0.131 from Refs. 11(d) and 11(e) whereas (21) leads to 0.1067; the exact numerical value is 0.1064 for $n=10$.

V. DISCUSSION

The analysis of the diagonalization of the matrix (4) conducted in this paper aimed at identifying the dynamical origin of the localization of eigenstates in regions of high potential energy, a phenomenon that appears widespread in chemical physics. Remarkable features of the numerically produced plots in Fig. 1 have been traced in Sec. III to the value of parameters of the matrix (4). Eigenvectors localized in the region of highest and lowest potential energy, with highest and lowest eigenvalues, are represented as superpositions of the *same small set of low-l orbitals,* mutually orthogonalized by the *conjugation transformation* (25). This orthogonalization combines with the general mutual repulsion of eigenvalues of a matrix to provide a quantum-dynamical basis for localization in high-potential regions. Analogies of states localized in high and low potentials had been apparent but their intimate conjugation relation seems to have been overlooked thus far.

A close analog of our results is seen in the long-known quantum mechanics of the asymmetric rotor, whose spectrum includes two groups of eigenstates localized about the axes of lowest and highest inertia, respectively.[22] The rotor's Hamiltonian matrix is tridiagonal in the base of symmetric-rotor eigenfunctions, the asymmetry being manifested by off-diagonal elements. The ratios of the intermediate to the highest and lowest moments of inertia determine the structure of the eigenvalue spectrum much as the values of $\mathcal{V}_l$ do in (4a). The rotor's eigenfunctions, Lamé elliptic functions of the orientation of a lab axis in the body frame, are changed into their complex conjugates by the analog of (25).

The results reported here are viewed as a stepping stone toward a semianalytic treatment of Rydberg and photoionization spectra in a magnetic field, involving the following tasks: (a) mapping of the perturbed eigenfunctions (1) and (31) so as to display their respective correlations of r and θ; a preliminary step has been taken in this direction;[23] (b) showing how and why the localized eigenfunctions of the degenerate perturbation treatment remain significant far beyond the validity of that treatment, as implied by Ref. 8; (c) describing the eventual decay of the quasi-Landau excitations, *transverse* to **B** and localized at $\theta \sim 90°$, into excitations (or ionizations) *along* **B**, i.e., localized at $\theta \sim 0°$. This program should probably clarify the interrelations between the fixed-n perturbation treatment, which correlates r and θ, the earlier adiabatic approach which excludes such correlations,[24] and a modified adiabatic approach that introduces correlations through adjustment of curvilinear coordinates.[25]

The present study is also intended as a stepping stone to the major class of problems of chemical physics that display hyperspherical symmetry in a Coulomb field about the center of mass and alternative symmetries near and beyond fragmentations, as well as resonances localized in high regions at intermediate ranges.[14,5] The departures from central symmetry at increasing distances from the center of mass introduce multivariable correlations akin to the correlations of r and θ considered here. Unraveling their multivariable aspect presents a new challenge.

ACKNOWLEDGMENTS

This work has been supported by the National Science Foundation through Grant Nos. PHY-86-10129 and PHY-86-07721 at The University of Chicago and Louisiana State University, respectively. One of us (A.R.P.R.) thanks Dr. Dana Browne for a helpful conversation and Dr. C. H. Greene for assistance in calculating Figs. 1 and 4.

APPENDIX: LINEAR STARK EFFECT IN A DEGENERATE MANIFOLD

The linear Stark effect in a degenerate hydrogenic manifold shares interesting similarities and differences with our problem of diamagnetism. This Stark problem is exactly solvable in accordance with the well-known separability in parabolic coordinates of the Hamiltonian for a

Coulomb plus electric field (**F** along the z direction),

$$H=-(1/r)+Fz \ . \tag{A1}$$

We use atomic units, a unit of F being 5.14×10^9 V/cm.

In the absence of parity as a good quantum number for (A1), all l values in the n manifold are mixed by this Hamiltonian. The mixing coefficients are Clebsch-Gordan coefficients that connect spherical to parabolic eigenvectors according to the prescription given by the O_4 symmetry of the hydrogen Hamiltonian.[26] With **L** the orbital angular momentum and **A** the Lenz vector (dimension of angular momentum), the combinations $\mathbf{j}_{1,2}=\frac{1}{2}(\mathbf{L}\pm\mathbf{A})$ behave like independent angular momenta. The parabolic states are described by $|j_1 j_2 j_{1z} j_{2z}\rangle$. The magnitudes of the two pseudoangular momenta are $j_1=j_2=\frac{1}{2}(n-1)$. Passage to spherical eigenvectors is accomplished by the addition $\mathbf{L}=\mathbf{j}_1+\mathbf{j}_2$. The eigenvalues of (A1) are equally spaced with spacing $3Fn$. The extreme eigenvectors (with energy $\pm\frac{3}{2}Fn^2$), with respective concentration of the wave function in the up- and down-field direction (along the positive-z and negative-z axis), are given for $m=0$ by the Clebsch-Gordan coefficient

$$\langle \tfrac{1}{2}(n-1),\tfrac{1}{2}(n-1),l,0 \mid \tfrac{1}{2}(n-1),\tfrac{1}{2}(n-1),\pm\tfrac{1}{2}(n-1),\tfrac{1}{2}(n-1)\rangle \ .$$

For $n\gg1$ and $n\gg l$, these coefficients equal[27]

$$P_l(\pm1)[(2l+1)/n]^{1/2}\exp[-l(l+1)/2n] \ . \tag{A2}$$

Examining this problem along the lines of the diamagnetism analysis in the text, the only nonvanishing matrix element of Fz is

$$W_l\equiv\langle n,l,0 \mid r\cos\theta \mid n,l+1,0\rangle$$
$$=\tfrac{3}{2}n^2\left[1-\left[\frac{l+1}{n}\right]^2\right]^{1/2}\frac{l+1}{[(2l+1)(2l+3)]^{1/2}} \ . \tag{A3}$$

The angular factor in this matrix element, $\langle l \mid \cos\theta \mid l+1\rangle$, is $1/\sqrt{3}$ for $l=0$ and $l\simeq1/2$ for all other l, a behavior similar to (2). Therefore W_l is well approximated for $l\neq0$ by

$$W_l\simeq\tfrac{3}{4}n^2\left[1-\frac{1}{2}\left[\frac{l+1}{n}\right]^2\right] , \tag{A4}$$

an expression analogous to (4b').

The $n\times n$ matrix of Fz has nonzero entries only along the two subdiagonals on either side of the main diagonal. The three-term recurrence relation in place of (6) is

$$W_{l-1}a_{l-1}+W_l a_{l+1}=Ea_l \ . \tag{A5}$$

The conjugation analogous to (24), $a_l=(-1)^l b_l$, switches the sign of the W_l's so that it takes the eigenvalue E into $-E$. Note that the absence of the diagonal elements now makes the transformation symmetric unlike in Sec. III C.

Analogous to (36) in Sec. IV, the difference equation (A5) with W_l as in (A4) can be mapped onto the differential equation in the variable $u=(l+\frac{1}{2})/n$,

$$[1-(u^2/2)]a''(u)-ua'(u)$$
$$+[(4E/3)+2n^2-n^2u^2]a(u)=0 \ , \tag{A6}$$

together with its conjugate wherein E is replaced by $-E$ and $a(u)$ by $b(u)$. These equations again describe prolate spheroidal functions. Their eigenvalues ascend and descend from the extreme values $E=\pm3n^2/2$, in equal steps of $3n$, with oscillator-type eigenfunctions. The extreme eigenvectors are as in (A2). As in Sec. III, the Gaussian falloff in l^2/n reflects the concentration of these wave functions at $\theta=0°$ and 180° with a Gaussian width $\sim n^{1/2}$.[27] Although these features and the association of the linear Stark effect with parabolic coordinates are well known, the above mapping of the problem onto prolate spheroidal functions, analogous to the diamagnetic problem, has not been recognized, nor has the role of the conjugation transformation.

[1] A. R. P. Rau, Phys. Rev. A **16**, 613 (1977).

[2] W. A. M. Blumberg, R. M. Jopson, and D. J. Larson, Phys. Rev. Lett. **40**, 1320 (1978); C. W. Clark, Phys. Rev. A **28**, 83 (1983); C. H. Greene, *ibid.* **28**, 2709 (1983).

[3] R. Garstang, Rep. Prog. Phys. **40**, 105 (1977).

[4] C. W. Clark, K. T. Lu, and A. F. Starace, in *Progress in Atomic Spectroscopy*, edited by H. J. Beyer and H. Kleinpoppen (Plenum, New York, 1984), Part C, p. 247.

[5] U. Fano, Phys. Rev. A **22**, 2660 (1980); *Atomic Physics*, edited by I. Lindgren *et al.* (Plenum, New York, 1983), Vol. 8, p. 5.

[6] C. W. Clark and K. T. Taylor, J. Phys. B **13**, L737 (1980); Nature **292**, 437 (1981).

[7] C. W. Clark, Phys. Rev. A **24**, 605 (1981); J. C. Gay, in Ref. 4, p. 177.

[8] D. Wintgen and H. Friedrich, J. Phys. B **19**, 1261 (1986).

[9] D. Wintgen and H. Friedrich, Phys. Rev. Lett. **57**, 571 (1986).

[10] A. Holle *et al.*, Phys. Rev. Lett. **56**, 2594 (1986); J. Main *et al.*, *ibid.* **57**, 2791 (1986).

[11] (a) E. A. Soloviev, Pis'ma Zh. Eksp. Teor. Fiz. **34**, 278 (1981) [JETP Lett. **34**, 265 (1981)]; (b) A. P. Kazantsev, V. L. Pokrovsky, and J. Bergou, Phys. Rev. A **28**, 3659 (1983); (c) P. A. Braun, Zh. Eksp. Teor. Phys. **84**, 850 (1983) [Sov. Phys—JETP **57**, 492 (1983)]; J. Phys. B **16**, 4323 (1983); (d) D. R. Herrick, Phys. Rev. A **26**, 323 (1981); (e) J. J. Labarthe, J. Phys. B **14**, 1467 (1981).

[12] M. L. Zimmerman, M. M. Kash, and D. Kleppner, Phys. Rev. Lett. **45**, 1082 (1980). This seminal paper diagonalized numerically the diamagnetic Hamiltonian matrix $(nl \mid H \mid n'l')$ *without* the restriction $n'=n$ but *with* truncated ranges of (n,n') and with varying field strength B. Its results showed a striking absence of widely avoided crossings between eigenvalues originating from different n at $B=0$, implying the ex-

istence at least of a quasiconstant of the motion besides the energy. They thus provided the empirical basis for the semianalytic extension of degenerate diagonalization in Ref. 8. They also displayed the peak density of eigenvalues at $\frac{1}{5}$ of the range of eigenvalues quasidiagonal in n, as noted by C. Goebel (unpublished).

[13]F. Robicheaux *et al.*, Phys. Rev. A **35**, 3619 (1987).

[14]U. Fano, Rep. Prog. Phys. **46**, 97 (1983); Phys. Rev. A **24**, 2402 (1981).

[15]L. Armstrong, Jr., Phys. Rev. A **3**, 1546 (1971).

[16]In multidimensional problems formulated in hyperspherical coordinates, Ref. 14, an analogous initial partition of a total quantum number would occur, $N=N_R+\lambda+1$, where λ labels the eigenvalues of a "grand angular momentum." The number λ can be partitioned in turn sequentially into further quantum numbers corresponding to angular variables. For example, the prototype treatment of two excited electrons has utilized a complete partition of λ indicated by $\lambda=l_1+l_2+2n_{rc}$, where l_1 and l_2 are orbital quantum numbers of the two electrons and n_{rc} pertains to their radial correlation. Each step of partition involves the variation of a quantum number from its lowest to its highest value, as l ranges in (5) from 0 to $n-1$ and $n_r=n-1-l$ ranges from $n-1$ to 0.

[17]The $\sum_N \varepsilon'_N$ over the eigenvalues of a Hermitian matrix M_{ik} is the trace of M^r, regardless of the diagonality of M. The trace of M^2 equals $\sum_{ik} |M_{ik}|^2$.

[18]The inaccuracy of this estimate is comparable to that obtained for a matrix accessible to exact treatment, namely, a tridiagonal $N\times N$ matrix with diagonal elements equal to 0 and off-diagonal equal to -1. For the rth eigenvector of this matrix we find the analog of (22) $NK^{(r)}=2N\sin(r\pi/2N)$, which reduces to the WKB value $r\pi$ only in the "continuous variable" limit $r/N\ll 1$. For $r/N\sim\frac{1}{3}$, as in our problem, the actual result $NK^{(N/3)}=N=(3/\pi)r\pi$ is low by 5%.

[19]See, e.g., L. Hoddeson, G. Baym, and M. Eckert, Rev. Mod. Phys. **59**, 287 (1987), Sec. II; also D. A. Browne *et al.*, Phys. Rev. B **30**, 5798 (1984).

[20]*Handbook of Mathematical Functions*, edited by M. Abramowitz and I. A. Stegun (Dover, New York, 1965).

[21]According to Ref. 13 the singularity of (36) at $u=\pi/2$ is taken into account by representing its solutions in the range of $u\sim\pi/2$ by

$$a(u)\sim\left[\frac{\pi}{2}-u\right]^{1/2}J_0\left[\frac{n}{\sqrt{5}}(4\varepsilon-1)^{1/2}\left[\frac{\pi}{2}-u\right]\right], \quad (34')$$

$$b(u)\sim\left[\frac{\pi}{2}-u\right]^{1/2}J_0\left[\frac{n}{\sqrt{5}}(1-4\varepsilon)^{1/2}\left[\frac{\pi}{2}-u\right]\right], \quad (34'')$$

where $J_0(x)$ is the zeroth-order Bessel function. The solution for the whole range of u is found by matching the logarithmic derivatives of this solution and of a Mathieu or analogous solution for smaller values of u.

[22]H. A. Kramers and G. P. Ittman, Z. Phys. **53**, 553 (1929); **58**, 217 (1929); **60**, 613 (1930).

[23]U. Fano, F. Robicheaux, and A. R. P. Rau, in *Abstracts of the Fifteenth International Conference on Electronic and Atomic Collisions, Brighton, U.K., 1987*, edited by J. Geddes, H. B. Gilbody, A. E. Kingston, and C. J. Latimer (Queen's University, Belfast, U.K., 1987). The correlation of r and θ implied by (1) and (31) is made explicit, conveniently, in terms of the WKB form of the radial hydrogenic functions, Eqs. 3.36 and 3.37 of H. A. Bethe and E. Salpeter, *Quantum Mechanics of One- and Two-Electron Atoms* (Springer, Berlin, 1957).

[24]A. F. Starace and G. L. Webster, Phys. Rev. A **19**, 1829 (1979).

[25]U. Fano, in *Semiclassical Descriptions of Atomic and Nuclear Collisions*, edited by J. Bang and J. de Boer (Elsevier, Amsterdam, 1985), p.367.

[26]L. D. Landau and E. M. Lifshitz, *Quantum Mechanics*, 3rd ed. (Pergamon, Oxford, 1977), pp. 131ff and 287ff.

[27]G. F. Drukarev, Zh. Eksp. Teor. Fiz. **83**, 946 (1982) [Sov. Phys.—JETP **56**, 532 (1982)]; A. R. P. Rau, J. Phys. B **17**, L75 (1984).